



## OPEN ACCESS

## EDITED BY

Qing-Lai Dang,  
Lakehead University, Canada

## REVIEWED BY

Rongzhou Man,  
Ontario Ministry of Northern  
Development, Mines, Natural  
Resources and Forestry, Canada  
Pengxin Lu,  
Ontario Ministry of Natural Resources  
and Forestry, Canada

## \*CORRESPONDENCE

Huanjiang Wang  
wanghj@igsnr.ac.cn  
Junhu Dai  
daijh@igsnr.ac.cn

## SPECIALTY SECTION

This article was submitted to  
Forest Ecophysiology,  
a section of the journal  
Frontiers in Forests and Global Change

RECEIVED 04 October 2022

ACCEPTED 16 November 2022

PUBLISHED 30 November 2022

## CITATION

Hu Z, Lin S, Wang H and Dai J (2022)  
Seasonal variations of cold hardiness  
and dormancy depth in five  
temperate woody plants in China.  
*Front. For. Glob. Change* 5:1061191.  
doi: 10.3389/ffgc.2022.1061191

## COPYRIGHT

© 2022 Hu, Lin, Wang and Dai. This is  
an open-access article distributed  
under the terms of the [Creative  
Commons Attribution License \(CC BY\)](#).  
The use, distribution or reproduction in  
other forums is permitted, provided  
the original author(s) and the copyright  
owner(s) are credited and that the  
original publication in this journal is  
cited, in accordance with accepted  
academic practice. No use, distribution  
or reproduction is permitted which  
does not comply with these terms.

# Seasonal variations of cold hardiness and dormancy depth in five temperate woody plants in China

Zhi Hu<sup>1,2</sup>, Shaozhi Lin<sup>1,2</sup>, Huanjiang Wang<sup>1\*</sup> and Junhu Dai<sup>1,2,3\*</sup>

<sup>1</sup>Key Laboratory of Land Surface Pattern and Simulation, Institute of Geographic Sciences and Natural Resources Research, Chinese Academy of Sciences, Beijing, China, <sup>2</sup>University of Chinese Academy of Sciences, Beijing, China, <sup>3</sup>China–Pakistan Joint Research Center on Earth Sciences, Chinese Academy of Sciences–Higher Education Commission of Pakistan, Islamabad, Pakistan

Woody plant species in temperate regions must withstand a cold winter and freezing events through cold acclimation and dormancy in autumn and winter. However, how seasonal changes in dormancy depth and cold hardiness affect the frost risk of temperate species is unclear because few studies have assessed dormancy depth and cold hardiness simultaneously. In this study, an experiment was conducted to estimate the dormancy depth and cold hardiness of five common woody temperate plant species during the winter of 2018/2019 in Beijing, China. Twigs of each species were collected at different dates during winter and the timing of budburst was monitored under the same forcing conditions. The dormancy depth was quantified as growing degree day (GDD) requirements of spring events. Simultaneously, the cold hardiness of buds at each sampling date was determined based on the electrical conductivity of the holding solution. Two indices (chilling accumulation and cold hardiness index) were used to simulate the past dynamics of dormancy depth, spring phenology, and cold hardiness from 1952 to 2021. The maximum dormancy depth of the study species was observed between early October and early December, and thereafter decreased exponentially. The cold hardiness peaked in mid-winter (end of December) through cold acclimation and thereafter decreased in spring (deacclimation). During the past 70 years, the budburst date (first flowering date or first leaf date) of five species was estimated to have advanced significantly, and dormancy depth in early spring was predicted to have increased owing to the warming-associated decrease in chilling accumulation. However, cold hardiness has decreased because of weakened acclimation and accelerated deacclimation under a warming climate. The frost risk before and after budburst remained unchanged because of the reduction in occurrence and severity of low-temperature events and earlier late spring frosts. The present

methods could be generalized to estimate and predict the seasonal changes in dormancy depth and cold hardiness of temperate species in the context of climate change.

#### KEYWORDS

spring phenology, climate change, dormancy, cold hardiness, experiment

## Introduction

Perennial plants in a temperate region must adapt to a climate with significant seasonal variation so as to complete their growth and development processes. Cold temperatures in winter not only affect the metabolic processes of plants (Sakai and Weiser, 1973; Kreyling et al., 2015; Pardee et al., 2017) but also cause formation of intracellular ice crystals in plant tissues (Larcher, 2003) and may lead to cell death. To adapt to seasonal changes in climate, temperate plants have evolved specific developmental rhythms and phenology (Basler and Körner, 2014). Recent climatic changes have dramatically altered plant phenophases, such as leaf unfolding, flowering, and leaf senescence (Zohner and Renner, 2014; Ge et al., 2015; Menzel et al., 2020). With phenological change (e.g., earlier budburst), the risk of frost damage may increase accordingly (Hänninen and Tanino, 2011; Richardson et al., 2018). Therefore, quantifying the seasonal changes in dormancy depth and cold hardiness is important for accurately assessing the potential cold damage to plants under climate change.

To cope with freezing temperatures, temperate deciduous plants form terminal buds in autumn and enter a state of dormancy in winter, with no active growth and low metabolic activity (Anderson et al., 2010). There are two primary phases in the dormant period of buds (Junttila and Hänninen, 2012). Triggered by a shortening photoperiod and lowering temperatures in autumn, buds first enter a state of endodormancy, during which the onset of growth is prevented by endogenous signals (Lang et al., 1987). A prolonged exposure to chilling temperature could help to release endodormancy. When the chilling is fulfilled, buds reach a state of ecodormancy, in which budburst and spring growth are prevented by unfavorable environmental factors. Budburst occurs when ecodormant buds are exposed to forcing temperatures for a period of time.

Along with changes in status of dormancy are the changes in plant tolerance against freezing temperatures. Cold acclimation leads to the development of cold hardiness in plants. The shorter photoperiod in association with lower temperatures in autumn initiate and strengthen cold acclimation (e.g., Arora et al., 2003; Beck et al., 2004; Kalberer et al., 2006). Upon exposure to warmer temperatures in spring, plants lose the cold hardiness

acquired during acclimation by the process of deacclimation (Flynn and Wolkovich, 2018; Roeber et al., 2022).

Dormancy induction and cold acclimation in autumn are both driven by short photoperiods and low temperatures. However, seasonal changes in dormancy depth and cold hardiness may not be fully synchronized, because low temperatures in winter reduce dormancy depth but increase cold hardiness. The maximum dormancy depth may occur shortly after dormancy induction, whereas the maximum cold hardiness generally occurs during the coldest period of winter (Charrier et al., 2011). A warming climate may reduce the cold hardiness of plants and cause plants to be more sensitive to freezing temperatures (Tao et al., 2021). Other than freezing temperatures prior to budburst, the risk of cold damage after budburst (also known as false spring) may be altered due to the earlier budburst under a warming climate (Gu et al., 2008; Ault et al., 2013). Given that few studies have assessed dormancy depth and cold hardiness of temperate plants simultaneously, how seasonal changes in dormancy depth and cold hardiness affect frost risk is unclear.

In this study, a controlled experiment was conducted on five temperate deciduous plants in Beijing, China, during the winter of 2018/2019 to assess seasonal changes in dormancy depth and cold hardiness. Two bioclimatic indices (chilling accumulation and cold hardiness index) were used to describe the effects of environmental factors on dormancy depth and cold hardiness, respectively. The trends in dormancy depth and cold hardiness from 1952 to 2021 were estimated using the bioclimatic indices calculated from historical climate data. Furthermore, historical frost risk before and after budburst was determined using the estimated cold hardiness and budburst dates. The aims of this study were (1) to evaluate the seasonal variations in dormancy depth and cold hardiness in temperate plants and (2) to assess the risk of exposure of temperate species to frost events over the last seven decades.

## Materials and methods

### Study site and species investigated

Five deciduous broadleaved species of two trees (*Fraxinus chinensis* and *Salix babylonica*) and three shrubs (*Jasminum*

*nudiflorum*, *Forsythia suspensa*, and *Syringa oblata*), widely distributed in temperate regions of China, were selected for the study. The sampling site was located in the Olympic Forest Park in northern Beijing (40°01'3.00"N, 116°23'2.98"E). Meteorological data (daily minimum and maximum temperatures and precipitation) for the period 1951–2021 in the study area were obtained from the China Meteorological Data Service Center.<sup>1</sup> The annual mean temperature and annual total precipitation in Beijing are 12.47°C and 586.92 mm (average for 1981–2010), respectively, and a trend for significant warming in the study area over the past 70 years is apparent (Figure 1A).

Twigs of each species were collected from 8 October, 2018 to 26 March, 2019. To assess the seasonal change in dormancy depth, twigs were sampled every 3–4 days, resulting in 42 collections in total. Because the pre-treatment time for measuring cold hardiness was longer than that for estimating dormancy depth, separate samples for determination of cold hardiness were collected every 15–20 days, resulting in 10 collections in total (Figure 1B).

## Measurement of dormancy depth

Five individuals of each species were selected for measurement of dormancy depth. One twig (bearing winter buds) approximately 20–30 cm long was collected from each individual on each sampling date. Samples were transported to the laboratory immediately after collection. We placed five twigs from each species in a glass bottle (0.25 L) containing tap water and transferred the bottles to growth chambers (Ningbo Jiangnan Instrument Factory). The growth chambers were set to day/night temperatures of 25°C/15°C and a photoperiod of 14 h/10 h (light/dark) with a flux density of 100  $\mu\text{mol}\cdot\text{m}^{-2}\cdot\text{s}^{-1}$ . A tray filled with water was placed inside the growth chamber to ensure that the relative humidity was maintained at approximately 70%. To prevent blockage of the xylem in the twigs, the base of the stems was pruned, and the water in the bottles was replaced weekly.

The development of each twig was monitored every 2 days. The first leaf date (FLD) and first flowering date (FFD) were recorded. The FLD was defined as the date when at least one leaf in a twig was fully unfolded, corresponding to BBCH 11. The FFD was defined as the date when the first flower on a twig had fully opened, corresponding to BBCH 60 (Meier, 2001). We only investigated the first spring event of each species. For two species that flowered earlier than leaf unfolding (*J. nudiflorum* and *F. suspensa*), the FFD was recorded. For the other three species (*F. chinensis*, *S. babylonica*, and *S. oblata*), the FLD was recorded.

<sup>1</sup> <http://data.cma.cn/en>

The growing degree day (GDD) requirement of FFD or FLD in the growth chamber was used to represent the dormancy depth (Dantec et al., 2014) or to assess the relationship between chilling and GDD requirement (Laube et al., 2014). The GDD requirement was calculated as the accumulation of temperature greater than a certain threshold. For twigs sampled before 1 January, 2019, only the GDD in the growth chamber was calculated because the ambient temperature was below 5°C, whereas for twigs sampled after this date, the GDD already accumulated outdoors was also included. The equation used to calculate GDD was:

$$GDD_R = \begin{cases} \sum_{t=t_s}^{t_f} \max(T_g(t) - T_b, 0) & \text{if } t_s < t_1 \\ \sum_{t=t_1}^{t_s} \max(T_o(t) - T_b, 0) + \sum_{t=t_s}^{t_f} \max(T_g(t) - T_b) & \text{if } t_s \geq t_1 \end{cases} \quad (1)$$

where  $GDD_R$  represents the GDD requirement of FLD and FFD;  $t_1$  is the date when GDD starts to accumulate (1 January, 2019);  $t_s$  is the sampling date;  $t_f$  is the date of onset of FLD or FFD averaged from five twigs;  $T_o(t)$  is the daily mean temperature outdoors at date  $t$ ;  $T_g(t)$  is the daily mean temperature inside the growth chamber, which was 20.83°C based on the day/night temperature and photoperiod set in the growth chamber; and  $T_b$  is the threshold temperature for GDD, which was set at 5°C based on previous studies (Kramer, 1994; Peaucelle et al., 2019; Wang et al., 2020a). All twigs were observed for 55 days after the sampling date (corresponding to 871°C-days, i.e., the average GDD from January to May in Beijing).

To describe the seasonal variation in dormancy depth, the variation in  $GDD_R$  (average of five individuals per species) with sampling date was plotted. Based on the shape of the curve, an exponential function was used to fit the changes in  $GDD_R$  (after the date of deepest dormancy):

$$GDD_R = a + be^{-c \cdot \text{date}} \quad (2)$$

where  $a$ ,  $b$ , and  $c$  are parameters, and date is the number of days since 1 October, 2018. The parameters were estimated using the least-squares method.

## Bioclimatic index for dormancy depth

Previous studies showed that the  $GDD_R$  of spring events is associated with chilling accumulation (CA) during winter (Fu et al., 2014; Wang et al., 2020b). Therefore, CA can be used as a bioclimatic index of dormancy depth. CA was calculated with the equation:

$$CA = \sum_{t=t_0}^{t_s} \begin{cases} 1 & \text{if } T_o(t) \leq 5^\circ\text{C} \\ 0 & \text{if } T_o(t) > 5^\circ\text{C} \end{cases} \quad (3)$$

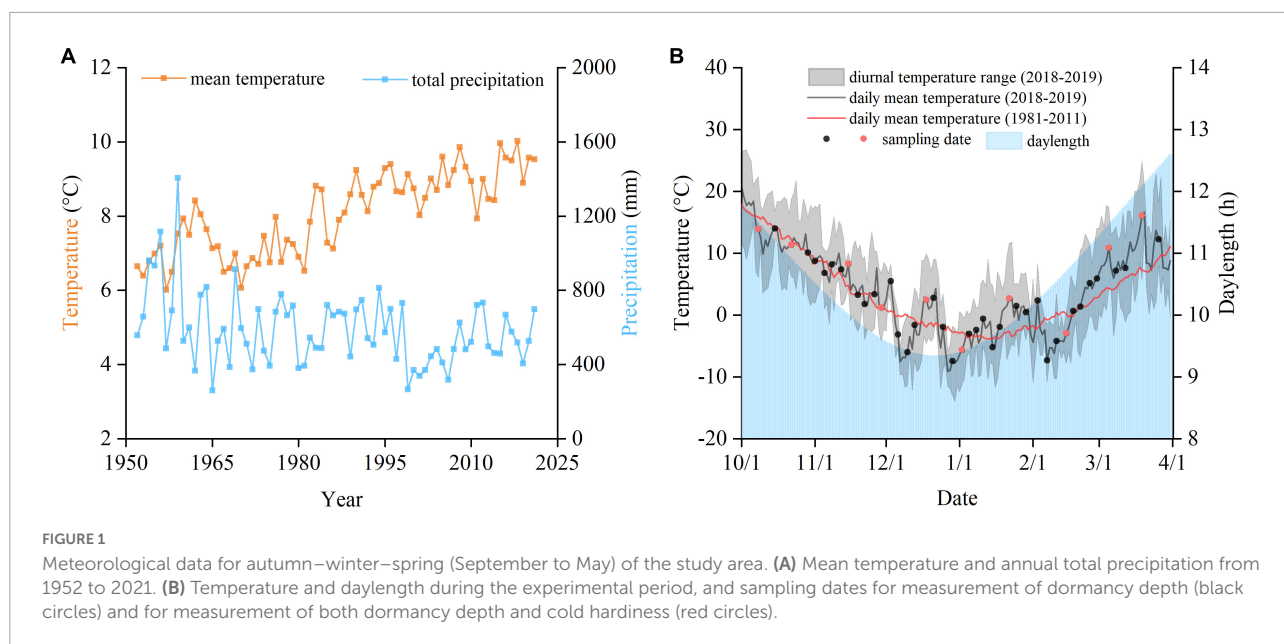


**TABLE 1** Target temperatures of each treatment at different sampling dates.

No.	Date	Target temperature (°C)					
1	8 October, 2018	5	−5	−10	−16	−22	−28
2	22 October, 2018	5	−8	−16	−22	−28	−35
3	15 November, 2018	5	−8	−16	−24	−32	−40
4	29 November, 2018	5	−8	−16	−24	−32	−40
5	18 December, 2018	5	−8	−16	−24	−32	−40
6	2 January, 2019	5	−8	−16	−24	−32	−40
7	22 January, 2019	5	−8	−16	−24	−32	−40
8	15 February, 2019	5	−8	−16	−24	−29	−35
9	5 March, 2019	5	−8	−16	−24	−28	−32
10	19 March, 2019	5	−5	−10	−16	−22	−28

where CA is the chilling accumulation.  $t_0$  is the date when CA started to accumulate (1 November, 2018),  $t_s$  is the sampling date.  $T_0(t)$  is the daily mean temperature at date  $t$ .

An exponential function between CA and  $GDD_R$  was established for each species:

$$GDD_R = a_1 + b_1 e^{-c_1^* CA} \tag{4}$$

where  $a_1$ ,  $b_1$ , and  $c_1$  are parameters estimated using the least-squares method.

### Measurement of cold hardiness

For each species, 30 twigs bearing dormant buds from 5 individuals were collected. The collected samples were randomly divided into six groups and preserved in plastic bags. The collected samples were first washed with deionized water. Subsequently, five groups were placed in programmable freezers

each maintained at a different target temperature, and one group was placed in a 5°C refrigerator (living control). The target temperatures of the five programmable freezers were adjusted according to the changes in cold hardiness (Table 1; Lenz et al., 2013; Vitasse et al., 2014; Vitra et al., 2017). All programmable freezers were cooled from 5°C at a rate of 6°C h<sup>-1</sup> until the target temperature was attained. The samples were kept at the target temperature for 4 h and then returned to 5°C at a rate of 6°C h<sup>-1</sup>. Finally, the dormant buds were removed from the twigs and placed in test tubes with 25 mL deionized water. The test tubes were placed in the refrigerator at 5°C for 24 h. The conductivity ( $S_1$ , i.e., electrolyte leakage after treatment) of the water in the test tubes was measured with a conductivity meter, and then the electrical conductivity ( $S$ ) was measured again after autoclaving the samples at 120°C for 30 min. The relative conductivity ( $E$ ) was calculated by combining the conductivity

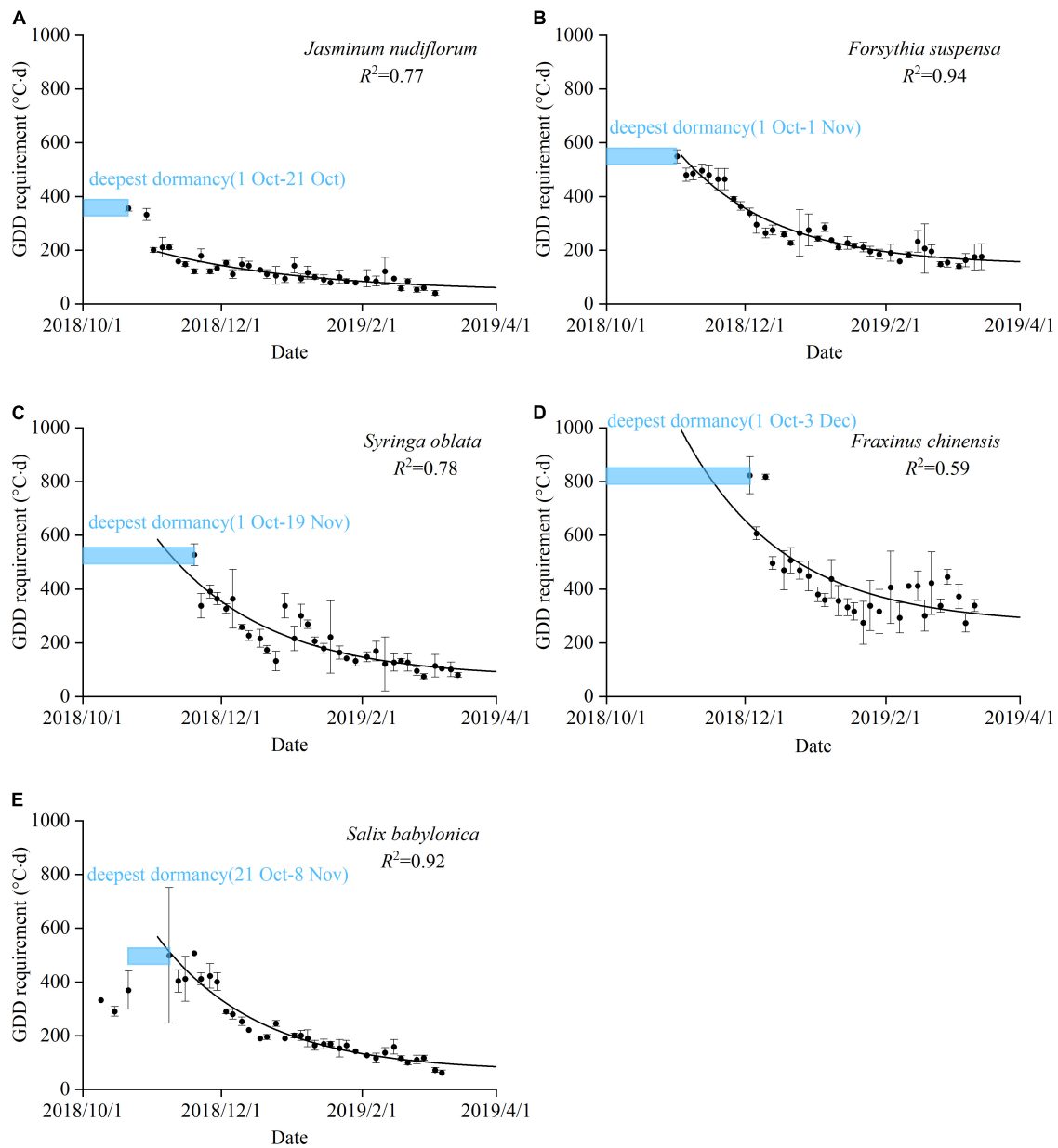


**FIGURE 2**  
 Seasonal variation in dormancy depth for five species. A blue box indicates the period of maximum dormancy depth, i.e., budburst did not occur even with sufficient growing degree days (GDD = 871°C·days, equivalent to the GDD from January to May in Beijing). Black dots: the GDD requirement (GDD<sub>R</sub>) of plants observed in the experiment. Error bars: standard deviation of five twigs. R<sup>2</sup>: coefficient of determination for the exponential function. (A) *J. nudiflorum*, (B) *F. suspensa*, (C) *S. oblata*, (D) *F. chinensis*, and (E) *S. babylonica*.

of deionized water ( $S_0$ ) with the following equation:

$$E = \left( \frac{S_1 - S_0}{S - S_0} \right) \times 100\% \quad (5)$$

The relationship between  $E$  and the target temperature ( $T$ ) was analyzed by logistic regression:

$$E(T) = \frac{K}{1 + i * e^{-j*T}} \quad (6)$$

where  $E(T)$  is the relative conductivity at temperature  $T$ , and  $i$ ,  $j$ , and  $K$  are model parameters. The temperature at a relative conductivity of 50%, i.e., the semi-lethal temperature (LT<sub>50</sub>), represents cold hardiness (Vitasse et al., 2014).

To describe the seasonal variation in cold hardiness, the cold hardiness (LT<sub>50</sub>) of each species (averaged from five individuals) with sampling dates was plotted. Because the cold hardiness initially increased and thereafter decreased during the study

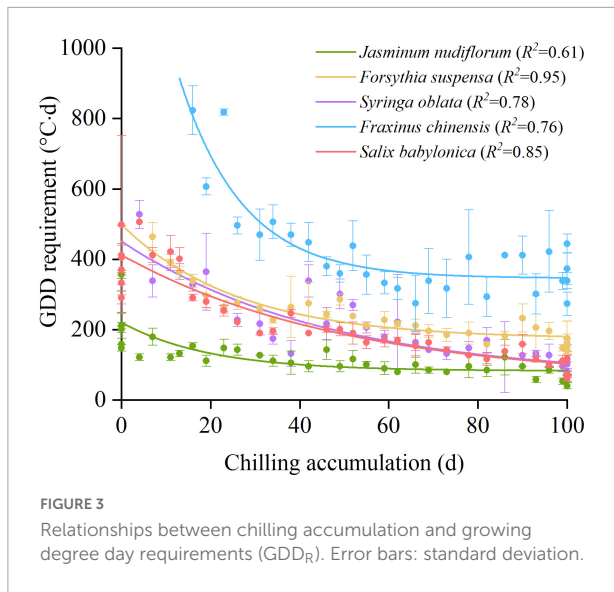


FIGURE 3 Relationships between chilling accumulation and growing degree day requirements (GDD<sub>R</sub>). Error bars: standard deviation.

period, a double logistic function was used to fit the curves:

$$y(x) = k_0 \left( \frac{1}{1 + e^{-k_1(x-50)}} + \frac{1}{1 + e^{k_2(x-120)}} - 1 \right) \quad (7)$$

where  $x$  is the sampling date,  $y$  is the cold hardiness at date  $x$ , and  $k_0$ ,  $k_1$ , and  $k_2$  are parameters estimated using a least-squares method.

### Bioclimatic index for cold hardiness

To simulate the seasonal variation in cold hardiness, the cold hardiness model proposed by Leinonen (1996) was modified and a normalized cold hardiness index (CHI) was constructed. CHI = 0 represents the lowest cold hardiness and CHI = 1 represents the strongest cold hardiness. We use  $[R(t)]$  to represent the CHI on day  $t$ .  $[R(t)]$  on day  $t$  depends on the CHI on the preceding day  $[R(t - 1)]$ , the potential cold hardiness on day  $t$   $[R_c(t)]$  and on day  $t - 1$   $[R_c(t - 1)]$ :

$$R(t) = R(t - 1) + \frac{1}{w} [R_c(t) - R_c(t - 1)] \quad (8)$$

where  $w$  is the weight of potential cold hardiness  $R_c(t)$  on actual cold hardiness.  $w$  was set to 5, because the  $R(t)$  corresponded better with the measured cold hardiness when  $w = 5$  compared with other values (2, 3, 4, and 6, 7, 8). The calculation of CHI started on 1 October. Because the outdoor temperature was still approximately 18°C on 1 October, it was assumed that cold acclimation had not started yet. The  $R(t)$  on 1 October was set to its minimum value (zero), and then  $R(t)$  on the next day was calculated with a daily scale.

The potential cold hardiness  $[R_c(t)]$  was determined by the effect of temperature  $[R_T(t)]$ , the effect of photoperiod  $[R_p(t)]$ , and hardening capacity ( $C_R$ ). The process of cold

acclimation before the winter solstice is driven by temperature and photoperiod (Kalberer et al., 2007), whereas deacclimation is mainly driven by temperature (Leinonen et al., 1997). Therefore,  $R_c(t)$  was calculated as:

$$R_c(t) = \begin{cases} C_R \times \frac{R_T(t)+R_p(t)}{2} & t \leq \text{winter solstice} \\ C_R \times \frac{R_T(t)+1}{2} & t > \text{winter solstice} \end{cases} \quad (9)$$

where  $R_T(t)$  is the effect of temperature on cold hardiness, and  $R_p(t)$  is the effect of photoperiod on cold hardiness. The equations for calculation of  $R_T(t)$  and  $R_p(t)$  are:

$$R_T(t) = \begin{cases} 1 - \frac{T(t)-T_{low}}{T_{up}-T_{low}} & \text{else} \\ 0 & T(t) > T_{up} \\ 1 & T(t) < T_{low} \end{cases} \quad (10)$$

where  $T_{up}$  is the maximum temperature limit, which was set to 10°C,  $T_{low}$  is the minimum temperature limit, which was set to -16°C (Leinonen, 1996), and  $T(t)$  is the daily mean temperature on date  $t$ .

$$R_p(t) = \begin{cases} 1 - \frac{P(t)-P_{low}}{P_{up}-P_{low}} & \text{else} \\ 0 & P(t) > P_{up} \\ 1 & P(t) < P_{low} \end{cases} \quad (11)$$

where  $P_{up}$  is the maximum daylength limit, which was set to 14 h,  $P_{low}$  is the minimum daylength limit, which was set to 8 h, and  $P(t)$  is the photoperiod on date  $t$ , which is calculated based on the latitude and the day of the year (Forsythe et al., 1995).

$C_R$  is assumed to increase linearly from 1 October to the winter solstice and thereafter decrease linearly from 1 to 0 from the winter solstice to the onset of spring events. Thus, the equation for calculation of  $C_R$  is:

$$C_R = \begin{cases} 0.2 \text{ to } 1 & \text{1st Oct} \leq t \leq \text{winter solstice} \\ 1 \text{ to } 0 & \text{winter solstice} < t \leq \text{spring event} \end{cases} \quad (12)$$

Regarding the initial value of  $C_R$  on 1 October, a set of values (0, 0.1, 0.2, 0.3, and 0.4) were tested, and the correlation coefficient between CHI and measured cold hardiness was largest at  $C_R = 0.2$ . Therefore, the initial value of  $C_R$  was set to 0.2.

After calculation of the daily CHI for each species, a linear regression model was calibrated to simulate cold hardiness (CH):

$$CH = m^*CHI + n \quad (13)$$

where  $m$  is the slope and  $n$  is the intercept, estimated with the least squares method. CH is the cold hardiness measured in the experiment. CHI is the daily cold hardiness index  $[R(t)]$ .

### Simulation of past changes in dormancy depth and cold hardiness

Using the daily mean temperature data during 1952–2021, CA from 1 November to each day until the end of April was

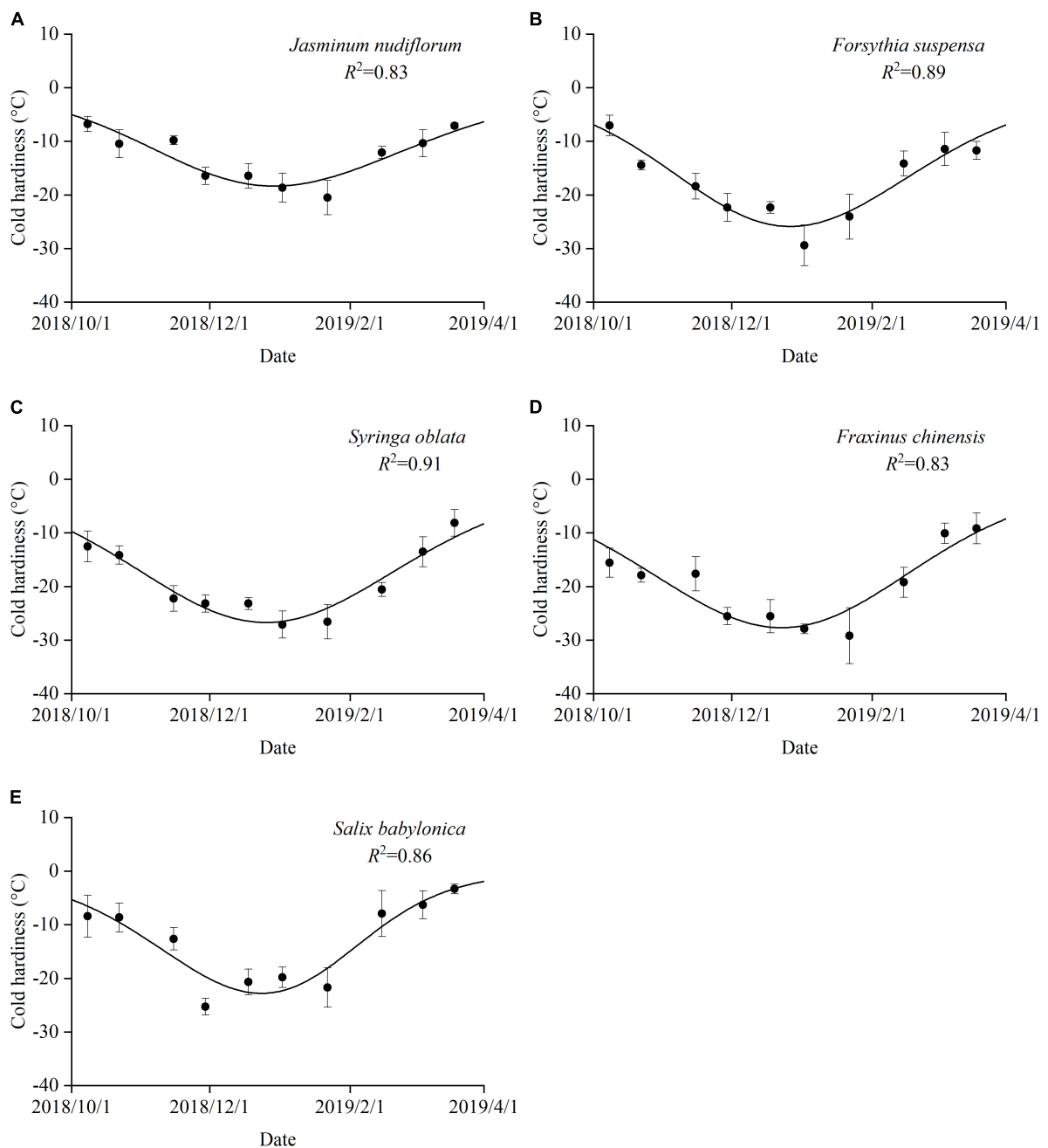


**FIGURE 4**  
Seasonal variations in cold hardiness for five species. Error bars: standard deviation.  $R^2$ : coefficient of determination for the double logistic function. (A) *J. nudiflorum*, (B) *F. suspensa*, (C) *S. oblata*, (D) *F. chinensis*, and (E) *S. babylonica*.

calculated for each species based on Equation 3. The course of dormancy depth ( $GDD_R$ ) over the last 70 years was estimated through Equation 4, and the interannual spring phenology was simulated as the date when  $GDD_R$  was attained. We also obtained the long-term FLD and FFD data of five species in Beijing from the China Phenological Observation Network (CPON) during 1963–2018. The historical phenological data

were collected at the Summer Palace, about 12 km from the sampling site of the experiment. We compared the simulated spring phenology with the long-term observed data to verify the robustness of phenological simulation.

The daily CHI from 1 October to 30 April was calculated for each year and Equation 13 was used to transform CHI into cold hardiness of each species. Finally, the interannual changes

in dormancy depth (on 1 March, because after this date the daily mean temperature is always  $>5^{\circ}\text{C}$ ) and maximum cold hardiness were analyzed.

## Simulation of historical frost events

Based on the simulated cold hardiness, we identified historical frost events (1952–2021) from the previous winter (1 November) to spring as the dates when daily minimum temperatures equal or below the estimated cold hardiness.

Furthermore, we adopted a widely used false spring index (FSI) to quantify the likelihood of damage to occur after budburst (Marino et al., 2011; Chamberlain et al., 2019).

$$FSI = LFD - BBD \quad (14)$$

where LFD is the last frost date in spring (the last day when daily minimum temperature  $<-2.2^{\circ}\text{C}$ ). BBD represents the budburst date, i.e., FLD or FFD of each species. Negative values indicate no-risk situations, whereas a positive FSI indicates cold damage occurred to young flowers or leaves.

## Results

### Seasonal changes of dormancy depth with chilling accumulation

For most species, budburst did not occur in the earliest-collected samples with sufficient GDD ( $871^{\circ}\text{C}\cdot\text{days}$ , equivalent to the outdoor GDD from January to May in Beijing), indicating that the twigs were in the maximum dormancy. For *S. babylonica*, the samples collected before 21 October underwent budburst, indicating that dormancy induction was not complete. However, budburst failed to occur in the samples collected between 21 October and 8 November, indicating that the buds entered deep dormancy during this period. Overall, maximum dormancy depth generally occurred between 1 October and 3 December. Thereafter, all species showed a clear exponential decrease in dormancy depth (Figure 2). An exponential function was used to fit the change in  $\text{GDD}_R$  with sampling dates. This function simulated the variation in dormancy depth with  $R^2$  ranging from 0.59 (*F. chinensis*) to 0.94 (*F. suspensa*). Therefore, the exponential function accurately reflected the change in dormancy depth over time.

The CA was correlated negatively and exponentially with  $\text{GDD}_R$  (Figure 3). For all species, the  $\text{GDD}_R$  decreased rapidly with increase in CA. However, when CA attained a certain threshold, the effect of CA on  $\text{GDD}_R$  decreased. The  $R^2$  of the exponential function between  $\text{GDD}_R$  and CA ranged from 0.61 to 0.95, indicating that CA was a good indicator of dormancy depth.

### Seasonal changes of cold hardiness with cold hardiness index

The cold hardiness of all species initially increased from autumn to mid-winter and thereafter decreased from mid-winter to spring (Figure 4). The maximum cold hardiness was observed between 29 November (*S. babylonica*) and 22 January (*J. nudiflorum* and *F. chinensis*). *F. chinensis* had the strongest cold hardiness of  $-11.45^{\circ}\text{C}$  on 1 October, which increased to  $-27.68^{\circ}\text{C}$  on 23 December. *Jasminum nudiflorum* had the weakest cold hardiness of  $-5.16^{\circ}\text{C}$  on 1 October, which only increased to  $-18.34^{\circ}\text{C}$  on 30 December. The temporal variation in cold hardiness for the five species was expressed by a double logistic function with  $R^2$  ranging from 0.83 (*J. nudiflorum* and *F. chinensis*) to 0.91 (*S. oblata*). The maximum cold hardiness (Figure 4) was observed later than the maximum dormancy depth (Figure 2) for all species.

The cold hardiness measured by the electrical conductivity method was correlated significantly and negatively with CHI for all species (Figure 5). The Pearson correlation coefficients ( $r$ ) ranged from 0.82 (*S. babylonica*) to 0.93 (*F. suspensa*). In the processes of both cold acclimation and deacclimation, CHI corresponded well with cold hardiness, indicating that CHI may be used as an indicator of actual cold hardiness.

### Dormancy depth over the past 70 years

Over the past 70 years, the CA from the preceding 1 November to the mean date of spring events decreased significantly with a linear trend of  $3.0 \text{ days decade}^{-1}$  (Figure 6A). Accordingly, the  $\text{GDD}_R$  of spring events (on 1 March) significantly increased for all species, and ranged from  $0.06^{\circ}\text{C}\cdot\text{days decade}^{-1}$  (*J. nudiflorum*) to  $2.17^{\circ}\text{C}\cdot\text{days decade}^{-1}$  (*S. babylonica*) (Figures 6B–D). Therefore, dormancy depth in early spring increased in strength for all species in the context of climate warming.

### Maximum cold hardiness over the past 70 years

The maximum CHI showed a trend of significant decrease over time for all species (Figure 7A). The changes in cold hardiness were simulated by a linear regression function between CHI and the measured cold hardiness for each species (Figure 7B). All species showed a significant decrease in cold hardiness with trends ranging from  $0.22^{\circ}\text{C decade}^{-1}$  (*J. nudiflorum*) to  $0.39^{\circ}\text{C decade}^{-1}$  (*S. babylonica*). Therefore, the reduced duration and magnitude of low winter temperatures have weakened the cold hardiness of all species to varying degrees.



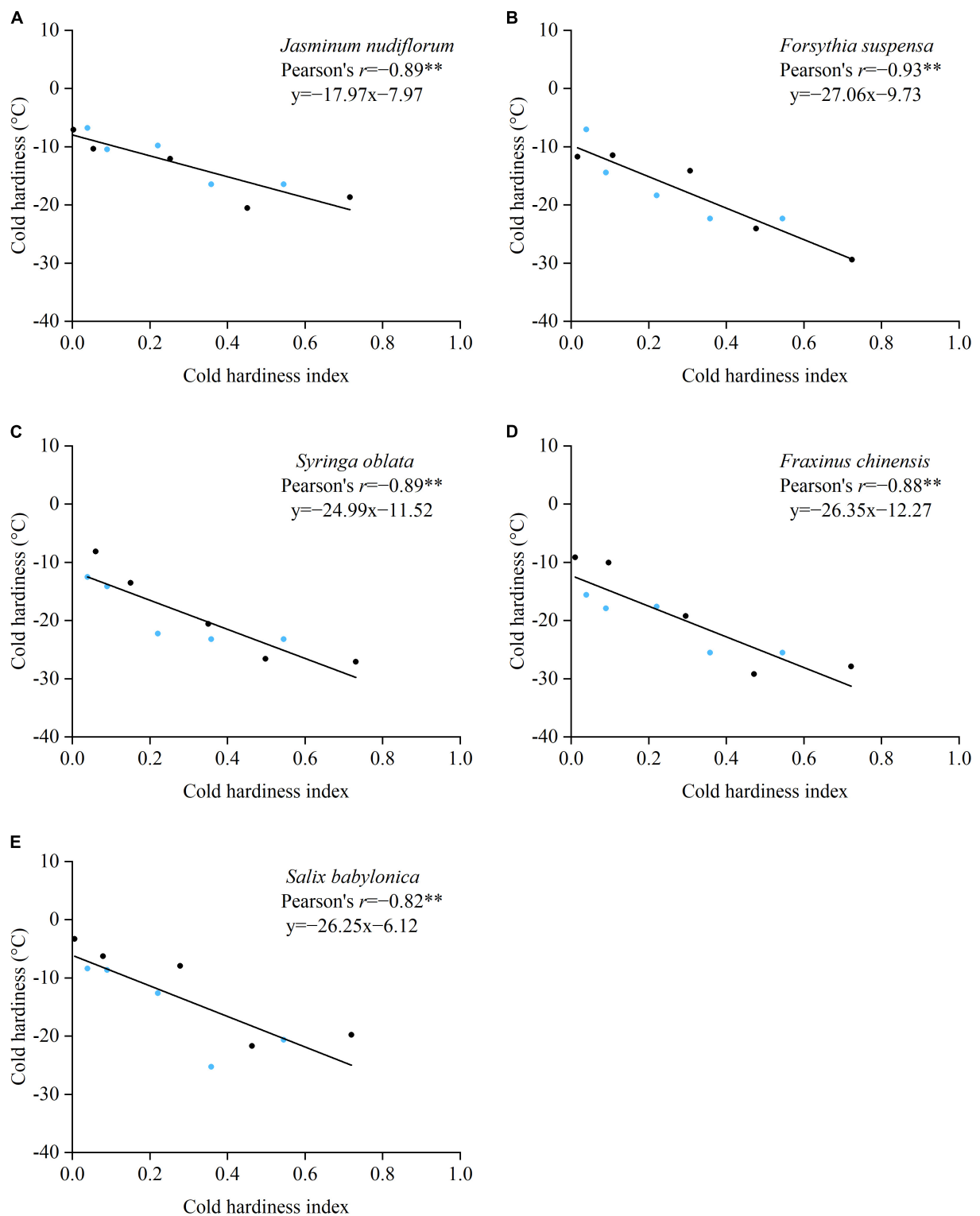
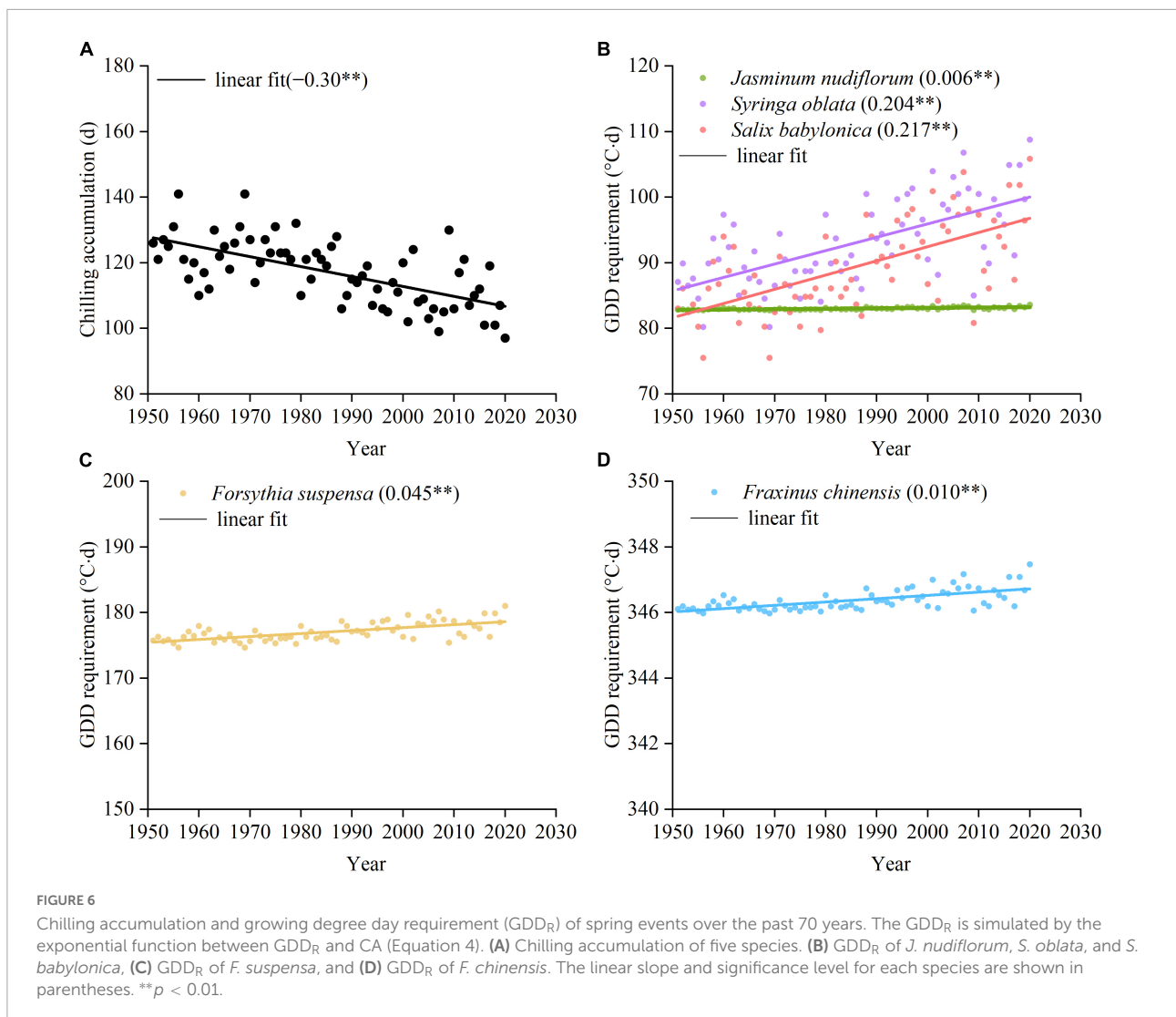


FIGURE 5

Relationships between cold hardiness measured with the electrical conductivity method and cold hardiness index estimated from Equation 8 for five species. Blue dots: samples in the process of cold acclimation. Black dots: samples in the process of deacclimation.  $**p < 0.01$ . (A) *J. nudiflorum*, (B) *F. suspensa*, (C) *S. oblata*, (D) *F. chinensis*, and (E) *S. babylonica*.



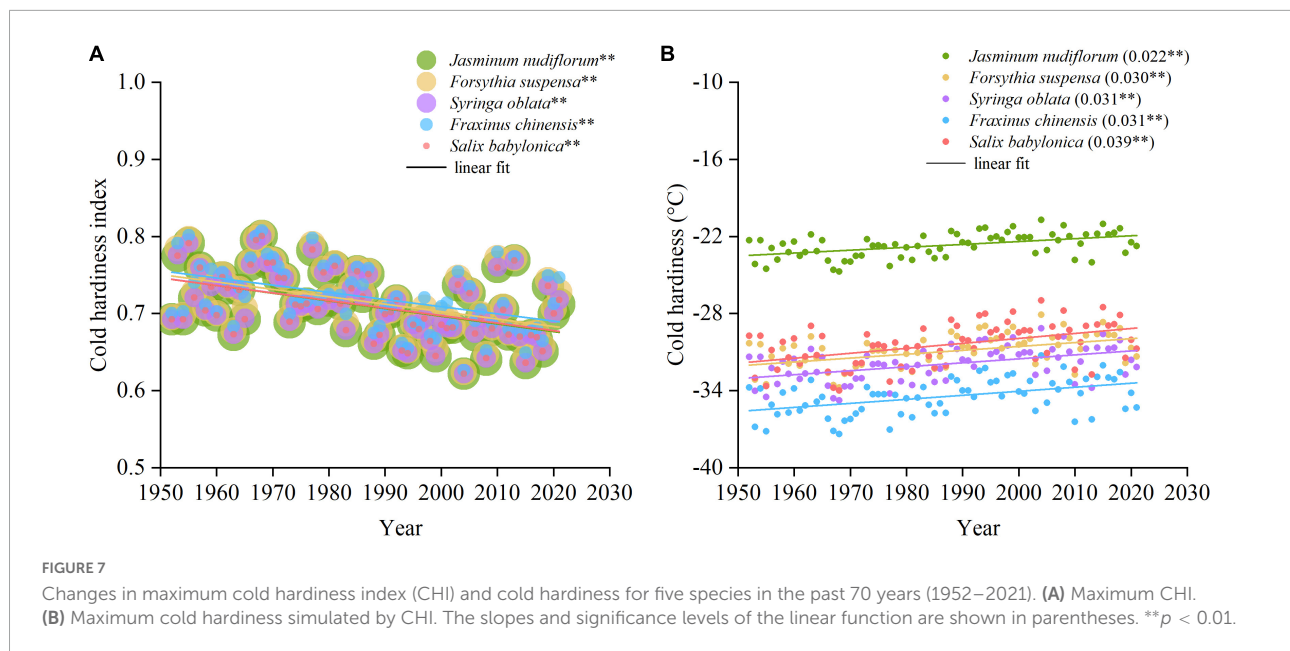
## Frost events in the past 70 years

To identify the historical frost events before or after budburst, we first simulated the annual FLD or FFD using the phenological model based on CA-GDD<sub>R</sub> functions. The results showed that the simulated budburst dates of five species advanced by 2.12 days decade<sup>-1</sup> to 2.44 days decade<sup>-1</sup> over the past 70 years (Supplementary Figure 1). Then, we validated the simulated spring phenology with the long-term observation data at a nearby site in Beijing. The results showed that the simulated spring phenology correlated positively and significantly with the observations (Figure 8), suggesting that the phenological models in this study well reflect the interannual changes in the spring phenology of all experimental species. However, the linear regression lines between the simulated and observed dates deviated from the 1:1 line for three species (*J. nudiflorum*, *F. suspensa* and *F. chinensis*), possibly because

of the phenological differentiation between populations and the difference in microclimate between two locations.

When comparing daily minimum temperatures and cold hardiness simulated by CHI, we found that the frost events before budburst rarely occurred in the past 70 years. Frost events only occurred several times in 4 years (1966, 1969, 1971, and 1979/1981) for *J. nudiflorum* and *S. babylonica*, but occurred only in one year (1966) for the other 3 species (Supplementary Table 1). Thus, the species investigated here have adapted to the seasonal temperature variation of the study area to a great extent.

We also assessed the post-budburst frost events in the past seven decades. The results showed that frost damage (positive FSI) only occurred in three species. Frost damage on young leaves or flowers occurred in 2, 1, and 1 years (all before 1970) on *J. nudiflorum*, *S. oblata* and *S. babylonica*, respectively (Figure 9). Furthermore, there were no significant trends in FSI due to the synchronous advance of the last



frost date and budburst date in response to climate warming (**Supplementary Figure 1**).

## Discussion

### Dormancy depth from winter to spring

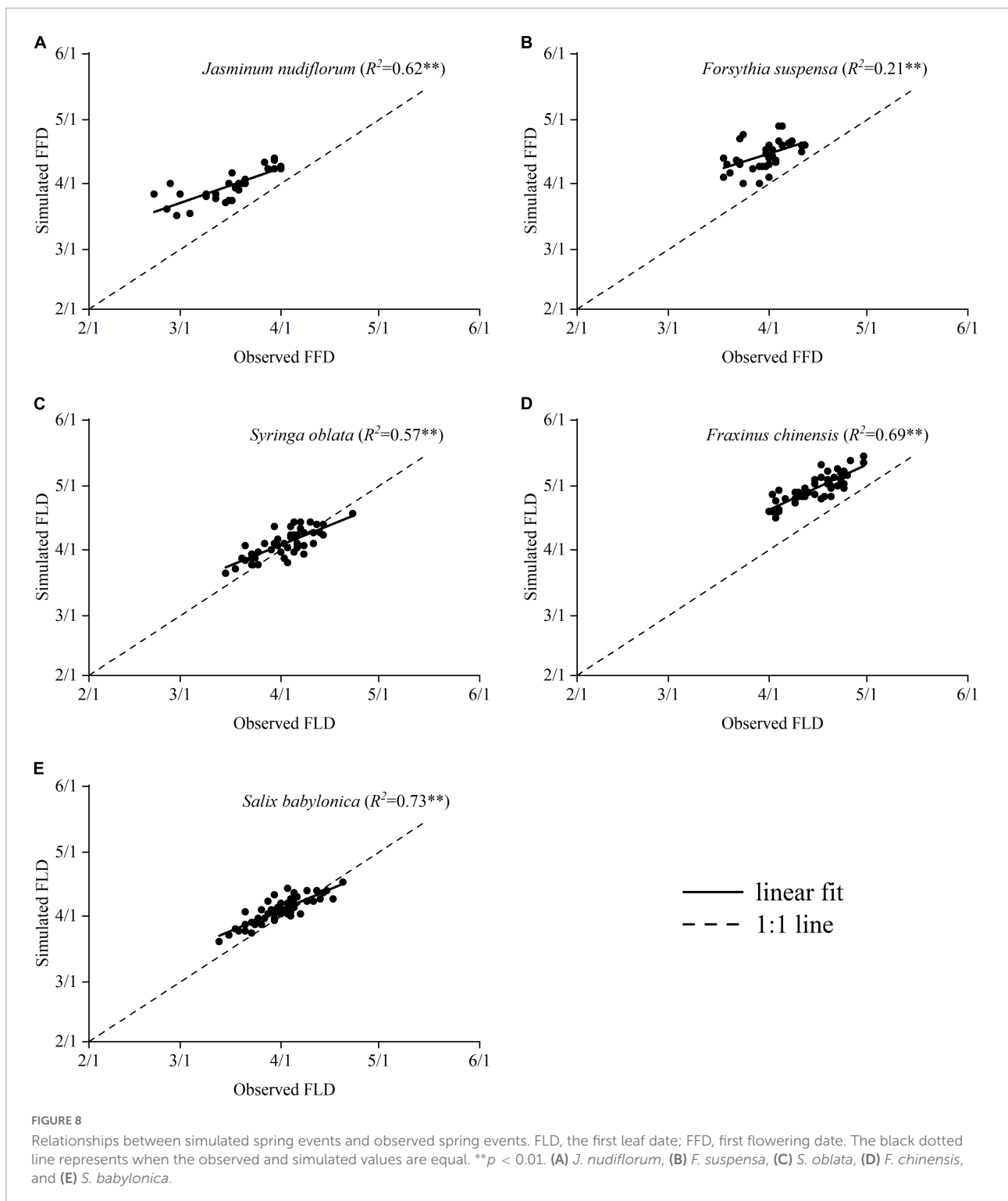
After endodormancy induced by the shortened daylength and lower temperatures in autumn, budburst in temperate trees and shrubs may not occur even in a growth-promoting environment (**Campoy et al., 2011; Basler and Körner, 2012; Singh et al., 2017**). In the present study, the maximum dormancy generally occurred between 1 October and 3 December for all five study species. This result is in accordance with previous findings. For example, the maximum dormancy depth of peach in Georgia, USA, was observed between late October and early December (**Weinberger, 1950**). Similarly, **Campoy et al. (2011)** reported that the maximum dormancy depth for apple usually occurred 1–2 months after the autumn equinox, which was consistent with the present results.

The release of endodormancy requires a certain amount of CA. In the current study, the dormancy level gradually decreased with increase in CA after plants attained the maximum dormancy. This result confirmed the effects of CA observed in previous studies. For example, the GDD requirements for budburst of seven temperate species gradually decrease with increase in chilling duration in Ontario, Canada (**Man et al., 2017**). The GDD requirement for budburst of European beech (*Fagus sylvatica*) is negatively correlated with duration of chilling (**Vitasse and Basler, 2013**). The effects of CA on dormancy depth are also evident in

observational data for 30 perennial species in Europe (**Wang et al., 2020b**). Although chilling plays a similar role in the dormancy release of temperate species, the different sensitivity of GDD requirements to CA among species may lead to varying phenological responses to climate warming (**Hu et al., 2022**).

### Cold hardiness from winter to spring

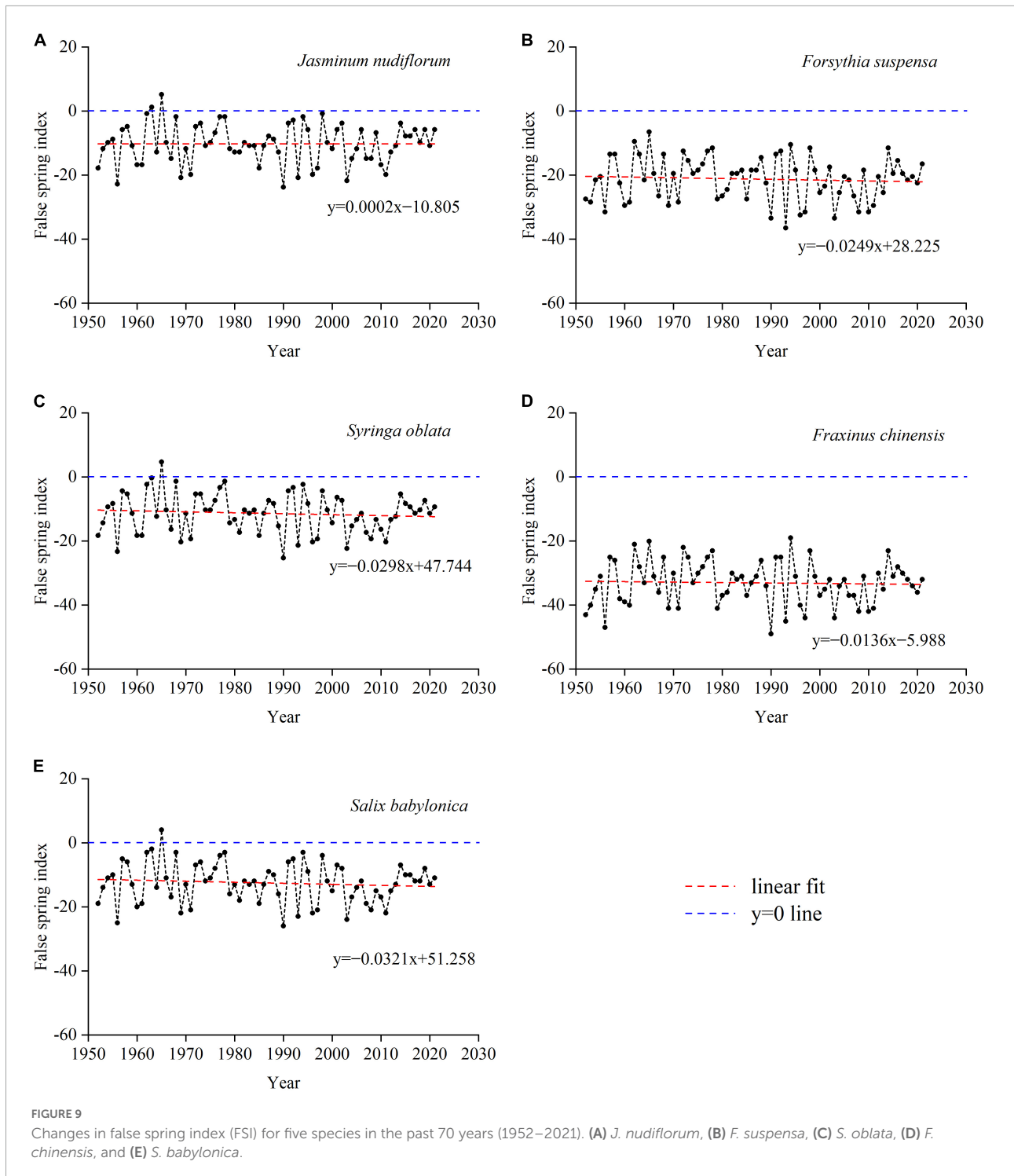
The cold hardiness of the five temperate species increased from the beginning of October, with the maximum cold hardiness observed at the end of December. This pattern has been reported in previous studies. For example, experiments on two Japanese cultivars of tea plant ('Yabukita' and 'Yutakamidori') in Kagoshima showed that cold hardiness gradually increases from the beginning of December to a maximum value in mid-February of the following year and thereafter steadily decreases (**Kimura et al., 2021**). The cold hardiness of twigs of 11 woody plant species at different altitudes in central France increases from early November to late winter (January–February) and then gradually decreases until budburst (**Charrier et al., 2013**). The cold hardiness of four woody plant species in Switzerland gradually decreases from the end of January to the beginning of April (**Vitra et al., 2017**). During the transition from autumn to winter, plant tissues start to harden owing to the decrease in temperature and the shortening of daylength (**Beck et al., 2004**), whereas cold deacclimation is mainly driven by progressively warmer temperatures in spring. Maximum cold hardiness differed among the five species, ranging between  $-18^{\circ}\text{C}$  and  $-28^{\circ}\text{C}$ , in the current investigation. The maximum cold hardiness



of fruit-oriented walnut can attain  $-28^{\circ}\text{C}$ , whereas that of wood-oriented walnut is  $-35^{\circ}\text{C}$  (Charrier et al., 2011). Nordic *Betula* species and other cold-adapted species can tolerate temperatures lower than  $-70^{\circ}\text{C}$  at full dormancy (Körner, 2012).

## Frost risk under climate change

The CA and CHI provided sufficient indications of seasonal variations in dormancy and cold hardiness. The present simulations indicated that dormancy depth is increasing owing



to decreased chilling. Similar results have been observed in previous studies. For instance, Wang et al. (2022) reported that insufficient chilling under climate warming has led to an increase in dormancy depth, which has approximately halved the rate of advance of spring phenology caused by increased forcing.

Temperate species with long life cycles have evolved the ability to cope with low seasonal temperatures within their distribution range. This explains why we detected very few frost events before budburst in the past 70 years (Supplementary Table 1). Since lower temperatures are more effective for cold acclimation, the present study simulated

a decrease in cold hardiness from the previous autumn to spring under climate warming. The decreased cold hardiness may cause a higher risk of frost damage. However, the occurrence of extremely low-temperature events decreased significantly under warming (Griffiths et al., 2005). Therefore, combined with decreased cold hardiness and frequency of low-temperature events, frost risk prior to budburst would not change significantly. The results of this study confirmed this assumption, as no frost events were simulated to occur in recent years.

The budburst date of temperate plants is now earlier owing to the influence of climate warming (Menzel et al., 2006; Ge et al., 2015). As a result, plants may be at increased risk of frost damage after budburst (Chamberlain et al., 2019). However, the earlier last frost date in a warmer climate tends to reduce the spring frost risk (Park et al., 2021). Thus, considering both the changes in spring phenology and the frequency of frost events, the post-budburst frost risk may vary among regions. This study found that the frost risk to young leaves and flowers did not change significantly. In Switzerland, the risk of spring frost exposure and subsequent potential damage has increased for four tree species at the vast majority of stations located at elevations higher than 800 m while remaining unchanged at lower elevations (Vitasse et al., 2018). A recent study showed that the frequency of frosts in late spring has increased to a greater extent in Europe and East Asia than in North America from 1959 to 2017 (Zohner et al., 2020).

## Conclusion

In this study, the dormancy depth and cold hardiness of five temperate woody plant species in Beijing were assessed from autumn to the following spring using growth chamber and conductivity measurements. The maximum dormancy occurred between early October and early December, which thereafter gradually decreased. The cold hardiness increased from the beginning of October until the end of December and thereafter decreased. The maximum dormancy and maximum cold hardiness were non-synchronized because of the different responses of dormancy and cold hardiness to low temperatures in winter. The bioclimatic indices CA and CHI satisfactorily represented seasonal changes in dormancy and cold hardiness, respectively. Using functions between CA and GDD requirements, the budburst date (FFD or FLD) of the five species was simulated to become significantly earlier and the dormancy depth in early spring was indicated to have increased owing to insufficient CA over the past 70 years. At the same time, winter warming has led to a significant reduction in cold hardiness. The frost risk before or after budburst remained stable because of the reduction in occurrence and severity of low-temperature events and

earlier late spring frosts. The experimental methods and bioclimatic indices proposed in this study may be used to simulate frost risk in other regions and under different climate-change scenarios.

## Data availability statement

The original contributions presented in this study are included in the article/Supplementary material, further inquiries can be directed to the corresponding authors.

## Author contributions

HW designed the study. ZH and HW performed the experiment, and wrote the manuscript. ZH and SL analyzed the data. JD revised the manuscript. All authors contributed to the article and approved the submitted version.

## Funding

This work was funded by the National Natural Science Foundation of China (Grant No. 41871032) and the National Key R&D Program of China (Grant No. 2018YFA0606102).

## Conflict of interest

The authors declare that the research was conducted in the absence of any commercial or financial relationships that could be construed as a potential conflict of interest.

## Publisher's note

All claims expressed in this article are solely those of the authors and do not necessarily represent those of their affiliated organizations, or those of the publisher, the editors and the reviewers. Any product that may be evaluated in this article, or claim that may be made by its manufacturer, is not guaranteed or endorsed by the publisher.

## Supplementary material

The Supplementary Material for this article can be found online at: <https://www.frontiersin.org/articles/10.3389/ffgc.2022.1061191/full#supplementary-material>

## References

- Anderson, J. V., Horvath, D. P., Chao, W. S., and Foley, M. E. (2010). "Bud dormancy in perennial plants: a mechanism for survival," in *Dormancy and Resistance in Harsh Environments*, eds E. Lubzens, J. Cerda, and M. Clark (Berlin: Springer), 69–90. doi: 10.1007/978-3-642-12422-8
- Arora, R., Rowland, L. J., and Tanino, K. (2003). Induction and release of bud dormancy in woody perennials: a science comes of age. *HortScience* 38, 911–921. doi: 10.21273/hortsci.38.5.911
- Ault, T. R., Henebry, G. M., De Beurs, K. M., Schwartz, M. D., Betancourt, J. L., and Moore, D. (2013). The false spring of 2012, earliest in North American record. *EOS* 94, 181–182. doi: 10.1002/2013EO200001
- Basler, D., and Körner, C. (2012). Photoperiod sensitivity of bud burst in 14 temperate forest tree species. *Agric. For. Meteorol.* 165, 73–81. doi: 10.1016/j.agrformet.2012.06.001
- Basler, D., and Körner, C. (2014). Photoperiod and temperature responses of bud swelling and bud burst in four temperate forest tree species. *Tree Physiol.* 34, 377–388. doi: 10.1093/treephys/tpu021
- Beck, E. H., Heim, R., and Hansen, J. (2004). Plant resistance to cold stress: mechanisms and environmental signals triggering frost hardening and dehardening. *J. Biosci.* 29, 449–459. doi: 10.1007/BF02712118
- Campoy, J. A., Ruiz, D., and Egea, J. (2011). Dormancy in temperate fruit trees in a global warming context: a review. *Sci. Hortic.* 130, 357–372. doi: 10.1016/j.scienta.2011.07.011
- Chamberlain, C. J., Cook, B. I., García, de Cortázar-Atauri, I., and Wolkovich, E. M. (2019). Rethinking false spring risk. *Glob. Chang. Biol.* 25, 2209–2220. doi: 10.1111/gcb.14642
- Charrier, G., Bonhomme, M., Lacoine, A., and Améglio, T. (2011). Are budburst dates, dormancy and cold acclimation in walnut trees (*Juglans regia* L.) under mainly genotypic or environmental control? *Int. J. Biometeorol.* 55, 763–774. doi: 10.1007/s00484-011-0470-1
- Charrier, G., Cochard, H., and Améglio, T. (2013). Evaluation of the impact of frost resistances on potential altitudinal limit of trees. *Tree Physiol.* 33, 891–902. doi: 10.1093/treephys/tpu062
- Dantec, C. F., Vitasse, Y., Bonhomme, M., Louvet, J. M., Kremer, A., and Delzon, S. (2014). Chilling and heat requirements for leaf unfolding in European beech and sessile oak populations at the southern limit of their distribution range. *Int. J. Biometeorol.* 58, 1853–1864. doi: 10.1007/s00484-014-0787-7
- Flynn, D. F. B., and Wolkovich, E. M. (2018). Temperature and photoperiod drive spring phenology across all species in a temperate forest community. *New Phytol.* 219, 1353–1362. doi: 10.1111/nph.15232
- Forsythe, W. C., Rykiel, E. J., Stahl, R. S., Wu, H., and Schoolfield, R. M. (1995). A model comparison for daylength as a function of latitude and day of year. *Ecol. Modell.* 80, 87–95. doi: 10.1016/0304-3800(94)00034-F
- Fu, Y. H., Piao, S., Zhao, H., Jeong, S. J., Wang, X., Vitasse, Y., et al. (2014). Unexpected role of winter precipitation in determining heat requirement for spring vegetation green-up at northern middle and high latitudes. *Glob. Chang. Biol.* 20, 3743–3755. doi: 10.1111/gcb.12610
- Ge, Q., Wang, H., Rutishauser, T., and Dai, J. (2015). Phenological response to climate change in China: a meta-analysis. *Glob. Chang. Biol.* 21, 265–274. doi: 10.1111/gcb.12648
- Griffiths, G. M., Chambers, L. E., Haylock, M. R., Manton, M. J., Nicholls, N., Baek, H. J., et al. (2005). Change in mean temperature as a predictor of extreme temperature change in the Asia-Pacific region. *Int. J. Climatol.* 25, 1301–1330. doi: 10.1002/joc.1194
- Gu, L., Hanson, P. J., Post, W., Mac, Kaiser, D. P., Yang, B., et al. (2008). The 2007 eastern US spring freeze: Increased cold damage in a warming world? *Bioscience* 58, 253–262. doi: 10.1641/B580311
- Hänninen, H., and Tanino, K. (2011). Tree seasonality in a warming climate. *Trends Plant Sci.* 16, 412–416. doi: 10.1016/j.tplants.2011.05.001
- Hu, Z., Wang, H., Dai, J., Ge, Q., and Lin, S. (2022). Stronger spring phenological advance in future warming scenarios for temperate species with a lower chilling sensitivity. *Front. Plant Sci.* 13:830573. doi: 10.3389/fpls.2022.830573
- Junttila, O., and Hänninen, H. (2012). The minimum temperature for budburst in *Betula* depends on the state of dormancy. *Tree Physiol.* 32, 337–345. doi: 10.1093/treephys/tps010
- Kalberer, S. R., Arora, R., Leyva-Estrada, N., and Krebs, S. L. (2007). Cold hardiness of floral buds of deciduous azaleas: dehardening, rehardening, and endodormancy in late winter. *J. Am. Soc. Hortic. Sci.* 132, 73–79. doi: 10.21273/jashs.132.1.73
- Kalberer, S. R., Wisniewski, M., and Arora, R. (2006). Deacclimation and reacclimation of cold-hardy plants: current understanding and emerging concepts. *Plant Sci.* 171, 3–16. doi: 10.1016/j.plantsci.2006.02.013
- Kimura, K., Yasutake, D., Oki, T., Yoshida, K., and Kitano, M. (2021). Dynamic modelling of cold-hardiness in tea buds by imitating past temperature memory. *Ann. Bot.* 127, 317–326. doi: 10.1093/aob/mcaa197
- Körner, C. (2012). *Alpine Treelines: Functional Ecology of the Global High Elevation Tree Limits*. Basel: Springer Science & Business Media.
- Kramer, K. (1994). A modelling analysis of the effects of climatic warming on the probability of spring frost damage to tree species in The Netherlands and Germany. *Plant. Cell Environ.* 17, 367–377. doi: 10.1111/j.1365-3040.1994.tb00305.x
- Kreyling, J., Schmid, S., and Aas, G. (2015). Cold tolerance of tree species is related to the climate of their native ranges. *J. Biogeogr.* 42, 156–166. doi: 10.1111/jbi.12411
- Lang, G. A., Early, J. D., Martin, G. C., and Darnell, R. L. (1987). Endo-, para-, and ecodormancy: physiological terminology and classification for dormancy research. *HortScience* 22, 371–377.
- Larcher, W. (2003). *Physiological Plant Ecology*. Berlin: Springer.
- Laube, J., Sparks, T. H., Estrella, N., Höfler, J., Ankerst, D. P., and Menzel, A. (2014). Chilling outweighs photoperiod in preventing precocious spring development. *Glob. Chang. Biol.* 20, 170–182. doi: 10.1111/gcb.12360
- Leinonen, I. (1996). A simulation model for the annual frost hardiness and freeze damage of scots pine. *Ann. Bot.* 78, 687–693. doi: 10.1006/anno.1996.0178
- Leinonen, I., Repo, T., and Hänninen, H. (1997). Changing environmental effects on frost hardiness of scots pine during dehardening. *Ann. Bot.* 79, 133–138. doi: 10.1006/anno.1996.0321
- Lenz, A., Hoch, G., Vitasse, Y., and Körner, C. (2013). European deciduous trees exhibit similar safety margins against damage by spring freeze events along elevational gradients. *New Phytol.* 200, 1166–1175. doi: 10.1111/nph.12452
- Man, R., Lu, P., and Dang, Q. L. (2017). Insufficient chilling effects vary among boreal tree species and chilling duration. *Front. Plant Sci.* 8:1354. doi: 10.3389/fpls.2017.01354
- Marino, G. P., Kaiser, D. P., Gu, L., and Ricciuto, D. M. (2011). Reconstruction of false spring occurrences over the southeastern United States, 1901–2007: an increasing risk of spring freeze damage? *Environ. Res. Lett.* 6:024015. doi: 10.1088/1748-9326/6/2/024015
- Meier, U. (2001). *Growth Stages of Mono- and Dicotyledonous Plants: BBCH Monograph*, 2nd Edn. Berlin: Federal Biological Research Centre for Agriculture and Forestry.
- Menzel, A., Sparks, T. H., Estrella, N., Koch, E., Aaas, A., Ahas, R., et al. (2006). European phenological response to climate change matches the warming pattern. *Glob. Chang. Biol.* 12, 1969–1976. doi: 10.1111/j.1365-2486.2006.01193.x
- Menzel, A., Yuan, Y., Matiu, M., Sparks, T., Scheifinger, H., Gehrig, R., et al. (2020). Climate change fingerprints in recent European plant phenology. *Glob. Chang. Biol.* 26, 2599–2612. doi: 10.1111/gcb.15000
- Pardee, G. L., Inouye, D. W., and Irwin, R. E. (2017). Direct and indirect effects of episodic frost on plant growth and reproduction in subalpine wildflowers. *Glob. Chang. Biol.* 24, 848–857. doi: 10.1111/jghl.12426
- Park, I. W., Ramirez-Parada, T., and Mazer, S. J. (2021). Advancing frost dates have reduced frost risk among most North American angiosperms since 1980. *Glob. Chang. Biol.* 27, 165–176. doi: 10.1111/gcb.15380
- Peaucelle, M., Janssens, I. A., Stocker, B. D., Descals Ferrando, A., Fu, Y. H., Molowny-Horas, R., et al. (2019). Spatial variance of spring phenology in temperate deciduous forests is constrained by background climatic conditions. *Nat. Commun.* 10:5388. doi: 10.1038/s41467-019-13365-1
- Richardson, A. D., Hufkens, K., Milliman, T., Aubrecht, D. M., Furze, M. E., Seyednasrollah, B., et al. (2018). Ecosystem warming extends vegetation activity but heightens vulnerability to cold temperatures. *Nature* 560, 368–371. doi: 10.1038/s41586-018-0399-1
- Roeber, V. M., Schmülling, T., and Cortleven, A. (2022). The photoperiod?: handling and causing stress in plants. *Front. Plant Sci.* 12:781988. doi: 10.3389/fpls.2021.781988
- Sakai, A., and Weiser, C. J. (1973). Freezing resistance of trees in North America with reference to tree regions. *Ecology* 54, 118–126. doi: 10.2307/1934380
- Singh, R. K., Svystun, T., AlDahmash, B., Jönsson, A. M., and Bhalerao, R. P. (2017). Photoperiod- and temperature-mediated control of phenology in

trees – a molecular perspective. *New Phytol.* 213, 511–524. doi: 10.1111/nph.14346

Tao, Z., Xu, Y., Ge, Q., Dai, J., and Wang, H. (2021). Reduced frost hardiness in temperate woody species due to climate warming: a model-based analysis. *Clim. Change* 165:35. doi: 10.1007/s10584-021-03074-4

Vitasse, Y., and Basler, D. (2013). What role for photoperiod in the bud burst phenology of European beech. *Eur. J. For. Res.* 132, 1–8. doi: 10.1007/s10342-012-0661-2

Vitasse, Y., Lenz, A., and Körner, C. (2014). The interaction between freezing tolerance and phenology in temperate deciduous trees. *Front. Plant Sci.* 5:541. doi: 10.3389/fpls.2014.00541

Vitasse, Y., Schneider, L., Rixen, C., Christen, D., and Rebetez, M. (2018). Increase in the risk of exposure of forest and fruit trees to spring frosts at higher elevations in Switzerland over the last four decades. *Agric. For. Meteorol.* 248, 60–69. doi: 10.1016/j.agrformet.2017.09.005

Vitra, A., Lenz, A., and Vitasse, Y. (2017). Frost hardening and dehardening potential in temperate trees from winter to budburst. *New Phytol.* 216, 113–123. doi: 10.1111/nph.14698

Wang, H., Dai, J., Peñuelas, J., Ge, Q., Fu, Y. H., and Wu, C. (2022). Winter warming offsets one half of the spring warming effects on leaf unfolding. *Glob. Chang. Biol.* 28, 6033–6049. doi: 10.1111/gcb.16358

Wang, H., Wang, H., Ge, Q., and Dai, J. (2020a). The interactive effects of chilling, photoperiod, and forcing temperature on flowering phenology of temperate woody plants. *Front. Plant Sci.* 11:443. doi: 10.3389/fpls.2020.00443

Wang, H., Wu, C., Ciais, P., Peñuelas, J., Dai, J., Fu, Y., et al. (2020b). Overestimation of the effect of climatic warming on spring phenology due to misrepresentation of chilling. *Nat. Commun.* 11:4945. doi: 10.1038/s41467-020-18743-8

Weinberger, J. H. (1950). Chilling requirements of peach varieties. *Proc. Am. Soc. Horticultural Sci.* 56, 122–128.

Zohner, C. M., Mo, L., Renner, S. S., Svenning, J. C., Vitasse, Y., Benito, B. M., et al. (2020). Late-spring frost risk between 1959 and 2017 decreased in North America but increased in Europe and Asia. *Proc. Natl. Acad. Sci. U S A.* 117, 12192–12200. doi: 10.1073/pnas.1920816117

Zohner, C. M., and Renner, S. S. (2014). Common garden comparison of the leaf-out phenology of woody species from different native climates, combined with herbarium records, forecasts long-term change. *Ecol. Lett.* 17, 1016–1025. doi: 10.1111/ele.12308